Received: 1 April 2022 | Revised: 8 June 2022 | Accepted: 27 July 2022

DOI: 10.1002/asl.1127

RESEARCH ARTICLE

Atmospheric Science Letters RMetS

Error investigation of rain retrievals from disdrometer data using triple colocation

Clizia Annella[1] | **Vincenzo Capozzi**[1,2] | **Giannetta Fusco**[1] | **Giorgio Budillon**[1] | **Mario Montopoli**[2,3]

[1]Department of Science and Technology, University of Naples Parthenope, Napoli, Italy

[2]National Research Council of Italy, Institute of Atmospheric Sciences and Climate (CNR-ISAC), Rome, Italy

[3]Center of Excellence Telesensing of Environment and Model Prediction of Severe events (CETEMPS), University of L'Aquila, L'Aquila, Italy

Correspondence
Vincenzo Capozzi, Department of Science and Technology, University of Naples Parthenope, Napoli, 80143, Italy.
Email: vincenzo.capozzi@uniparthenope.it

Funding information
Optimization of nowcasting methods based on X-band weather radar and Provision of a service of weather forecasting to support the management of highway traffic on the A1 section from Caianello to Naples, on the A30 from Caserta to Salerno and on the A16 section from Naples to Candela, Grant/Award Number: Contract SAP n.81004904; AUTOSTRADE PER L'ITALIA (S.p.A.)

Abstract

Assessing the uncertainty of precipitation measurements is a challenging problem because precipitation estimates are inevitably influenced by various errors and environmental conditions. A way to characterize the error structure of coincident measurements is to use the triple colocation (TC) statistical method. Unlike more typical approaches, where measures are compared in pairs and one of the two is assumed error-free, TC has the enviable advantage to succeed in characterizing the uncertainties of co-located measurements being compared to each other, without requiring the knowledge of the true value which is often unknown. However, TC requires to have at least three co-located measuring systems and the compliance with several initial assumptions. In this work, for the first time, TC is applied to in-situ measurements of rain precipitation acquired by three co-located devices: a weighing rain gauge, a laser disdrometer and a bidimensional video disdrometer. Both parametric and nonparametric formulations of TC are implemented to derive the rainfall product precision associated with the three devices. While the parametric TC technique requires tighter constraints and explicit assumptions which may be violated causing some artifacts, the nonparametric formulation is more flexible and requires less strict constrains. For this reason, a comparison between the two TC formulations is also presented to investigate the impact of TC constrains and their possible violations. The results are obtained using a statistically robust dataset spanning a 1.5 year period collected in Switzerland and presented in terms of traditional metrics. According to triple colocation analysis, the two disdrometers outperform the classical weighing rain gauge and they have similar measurement error structure regardless of the integration time intervals.

KEYWORDS

disdrometer instruments, error analysis, rainfall estimation, triple colocation methods

1 | INTRODUCTION

It is well known that precipitation, being the principal player in the hydrological cycle and an important input in hydro-meteorological and climate models, plays a key role in human life and many fields of science. Nowadays, a wide suite of devices based on different technologies is available to measure precipitation (Kathiravelu et al., 2016; Tapiador et al., 2012; World Meteorological Organization, 2018). While rain gauges are considered the most traditional in-situ instruments for estimating rainfall amount and are practically ubiquitous, disdrometers are becoming popular, due to their ability in measuring the microphysical structure of precipitation (Adirosi et al., 2021; Marzano et al., 2010). However, both types of instruments may be subjected to several potential error sources, and except in case of controlled laboratory experiments, it is problematic to find an error-exempt reference against which to compare. A brilliant alternative to conduct error analysis is represented by the triple colocation statistical method (hereafter, TC), which requires the coexistence of three co-located measurements and provides a way to characterize errors, supposing the method assumptions are correct. TC has the additional advantage of being able to estimate the features of random error which characterize the three input observations without the need of a true reference. In this work, the traditional TC method (Alemohammad et al., 2015a) and an alternative nonparametric version (Nearing et al., 2017b) are adopted to derive the uncertainty of three popular devices for rainfall measurements: the OTT Pluvio^2 weighing rain gauge, the Thies Clima optical disdrometer and the bi-dimensional video disdrometer, hereafter named as RG, THCD and 2DVD, respectively. To date, the TC method has been involved in several studies focused on the comparison among remote-sensing precipitation estimates, reanalysis, and in-situ measurements (Alemohammad et al., 2015a; Duan et al., 2021; Li et al., 2018; Li et al., 2020; Massari et al., 2017). As far as the authors have been able to ascertain, this is the first time TC has been used to characterize the rain gauge and disdrometer errors. To meet this goal, the precipitation dataset discussed and analyzed in Fehlmann et al. (2020a) has been considered. The performances of RG, THCD, and 2DVD, have already been investigated in the past through the standard comparison approach, using a co-located pair of rainfall measuring devices (Fehlmann et al., 2020a; Lanzinger et al., 2006; Larsen et al., 2014). The results of the literature show there is still no clear direction in the characterization of errors in the disdrometric data, in which this study aims to contribute. The work is organized into five sections: Section 2 describes the available dataset in terms of RG, THCD, and 2DVD devices; Section 3 summarizes the TC formulations as well as the more standard dual co-location approach; Section 4 describes the processing applied to input data; Section 5 shows the results obtained; and in Section 6 the conclusions are drawn.

2 | AVAILABLE PRECIPITATION MEASUREMENTS

In this section, the three different devices of RG, THCD, and 2DVD, are briefly described. Their measurements are accessible in Fehlmann et al. (2020b) and refer to a dataset consisting of about 20,000 observations of rain precipitation sampled each minute, collected during the period from 1 November 2017 to 30 June 2019 in a pre-alpine site in Switzerland for a total of 607 days. The measuring site was characterized by very low wind conditions (values of mean, standard deviation, and maximum value during rain events are 0.4 m s^{-1}, 0.5 m s^{-1}, and 4.7 m s^{-1}, respectively), thus allowing to minimize the detrimental wind effects (Chinchella et al., 2021; Colli et al., 2018; Kruger & Krajewski, 2002).

2.1 | 2DVD disdrometer

The 2DVD, manufactured by Joanneum Research, is a sophisticated particle imaging system able to store detailed information, such as the shape, fall velocity, and equivalent diameter (D_j), including precise detection time (in ms), for each jth individual particle falling through a virtual measuring area of approximately 100 cm^2. The instrument consists of two high-speed line-scan cameras aligned orthogonally to each other and the 2DVD pre-processing considers only drops fully within the field of view of both systems. This results in a decrease of the sensing area as a function of drop sizes, called the effective measuring area. The 2DVD is generally considered quite reliable, even if some drawbacks have been noted (Raupach & Berne, 2015). In particular, the 2DVD proved to be unreliable in the measurements of drops smaller than 0.2 mm (Kruger & Krajewski, 2002). Moreover, some detection problems are related to the effects of wind turbulence, splashing, mismatching between cameras or external interference (e.g., insects or spiderwebs) which may cause measurement errors. To mitigate some of those artifacts, previous studies have applied a velocity filter to the data (Adirosi et al., 2014; Thurai & Bringi, 2005; Tokay et al., 2001). Consequently, drops exceeding ±50% of the expected terminal fall speed in Atlas et al. (1973) are removed.

The 2DVD rain rate is derived as the total flux flowing through the detection area of the instrument, that is, as the summation, over N detected drops, of the drop's spherical-equivalent volume ($\frac{\pi}{6}D_j^3$) per unit of time (ΔT) and effective sampling area (A_j) (Larsen & Blouin, 2020):

$$R_{2DVD}^{\Delta T} = \sum_{j=1}^{N} \frac{\frac{\pi}{6}D_j^3}{\Delta T A_j} \tag{1}$$

In Equation (1), the rain rate is in mm h^{-1} if ΔT, A_j and D_j are in hours, mm^2 and mm, respectively. Note that A_j and D_j are sampled by the 2DVD every 1 ms, but we calculated the rain rate setting $\Delta T = 1$ min thus obtaining $R_{\mathrm{2DVD}}^{1\,\mathrm{min}}$.

2.2 | Thies Clima disdrometer

The core element of THCD is an optical sensor, consisting of a parallel horizontal light beam of 0.75 mm thickness with a measuring area of approximately 45.6 cm^2. Particle sizes and vertical speeds are subdivided into 22 and 20 classes, respectively and, in each class (j,k), the count of the falling particles ($N_{j,k}$) is stored every minute together with the precipitation intensity, its amount and type (Clima, 2015). Thies Clima provides a more complete characterization of the precipitation with respect to traditional devices, although its measurements may be affected by some detection issues related to wind effects, double or partial drop detection (binning effect) and splashing (Capozzi et al., 2021; Chinchella et al., 2021). In order to remove spurious measurements, the same velocity filter used for the 2DVD is applied. The rainfall rate (mm h^{-1}) is derived similarly to Equation (1) from filtered Thies data by the following relationships (Angulo-Martínez et al., 2018):

$$R_{\mathrm{THCD}}^{\Delta T} = \sum_{j,k} \frac{\frac{\pi}{6}D_j^3 N_{j,k}}{\Delta T A_j} \tag{2}$$

$$A_j = A\left(1 - \frac{D_j}{2w}\right) \tag{3}$$

$R_{THCD}^{\Delta T}$ is in mm h^{-1} when ΔT, D_j and A_j are in hours, mm^2 and mm, respectively. In Equation (3), A is the physical sampling area of the disdrometer (45.6 cm^2), w is the width of the laser beam (20 mm) and A_j is the effective sampling area. From the perspective of the applicability of TC, discussed below, it should not be forgotten that sampling limitations due to binning effects, different detection areas and other sources of error are processed differently by 2DVD and THCD, leading to a different error structure introduced by these devices.

2.3 | Rain gauge

The OTT Pluvio^2 is a rain gauge that uses the balance principle to automatically determine the intensity and amount of precipitation with high-precision. Rain gauges have been used as ground references in several applications, although they are not exempted by some systematic errors due to wind and aerodynamic effects, wetting losses and surrounding environment (Colli et al., 2013, 2018; Saha et al., 2021). More specifically, OTT Pluvio^2 is able to recognize precipitation type (liquid or solid) and provides a raw precipitation value every 6 s by determining the weight of the collecting bucket. The data are then subjected to quality control to prevent incorrect measurements (e.g., due to wind, evaporation) and, depending on the type of algorithm used, two types of 1-min output are available: real-time and non-real-time product (OTT HydroMet GmbH, 2019). Since the operating instructions indicate the latter as being more accurate, in our study we selected the non-real-time product.

3 | ERROR ESTIMATION METHODS

This section presents a brief summary of both the traditional parametric and nonparametric TC formulation.

3.1 | Parametric triple colocation

In the parametric triple colocation (P-TC) with multiplicative error (Alemohammad et al., 2015a; Tian et al., 2013), each of the three spatially and temporally co-located measurements, X_i, with $i = 1, 2, 3$, are assumed to respect the following model:

$$X_i = \gamma_i T^{\beta_i} e^{\varepsilon_i} \tag{4}$$

where γ_i and β_i are the multiplicative and deformation errors, respectively, ε_i is a zero-mean random error, and T the unobserved true quantity. A few mathematical assumptions are required to comply for the P-TC method: (a) linearity (i.e., logarithmic form of Equation (4) should hold), (b) error orthogonality (i.e., independence of common signal T and noise ε_i), (c) error independence (i.e., ε_i terms are independent of each other), (d) stationarity (i.e., T and ε_i have constant mean and standard deviation with time) and (e) representativeness (i.e., the three measuring systems must observe the quantity T with similar geometrical properties). In the scenario considered in this study involving collocating measurements from 2DVD, THCD, and RG systems, it is reasonable to suppose the assumption in which (c) holds, since these are three devices based on a different detection system, and error sources are processed differently by the three devices (Johannsen et al., 2020; Kruger & Krajewski, 2002; Park et al., 2017). With regard to assumption (b), the fact that rain precipitation is a positive-only variable may lead to a violation of that assumption (Alemohammad et al., 2015a; Duan et al., 2021). Thus, to alleviate the impact of the error nonorthogonality issue, the aggregated time slots with null precipitation are filtered out as done in Alemohammad et al. (2015a) and Massari et al. (2017). Although such filtering procedure does not completely solve the error nonorthogonality issue, the presence of residual errors does not prevent the applicability of the P-TC, as recognized by Yilmaz and Crow (2014). Finally, the validity of the assumption (d) has been verified as in Caires and Sterl (2003) by testing the error variance estimates obtained in several time sub-intervals with those obtained from the entire dataset. In so doing, we found a low variation of the error variance with time which supports the validity of assumption (d).

Furthermore, after some mathematical manipulations (Gruber et al., 2015), we are able to calculate the error standard deviation (σ_{ε_i}) of the three measuring systems:

$$\sigma_{\varepsilon_1} = \sqrt{\sigma_1^2 - \frac{\sigma_{12}\sigma_{13}}{\sigma_{23}}} \tag{5a}$$

$$\sigma_{\varepsilon_2} = \sqrt{\sigma_2^2 - \frac{\sigma_{12}\sigma_{23}}{\sigma_{13}}} \tag{5b}$$

$$\sigma_{\varepsilon_3} = \sqrt{\sigma_3^2 - \frac{\sigma_{13}\sigma_{23}}{\sigma_{12}}} \tag{5c}$$

where σ_i^2 and σ_{ij} are the variance and the covariance of the input time series X_i and (X_i, X_j), respectively. Note that ε_i is zero-mean and, consequently, the terms σ_{ε_i} coincide with the root mean square error (RMSE) associated with each measuring system. A second output quantity provided by the P-TC is the the correlation coefficient ($\rho_{[T,i]}$) between the actual unobserved value T and each input time series X_i (Mccoll et al., 2014):

$$\rho_{(T,1)} = \sqrt{\frac{\sigma_{12}\sigma_{13}}{\sigma_{11}\sigma_{23}}} \tag{6a}$$

$$\rho_{(T,2)} = \sqrt{\frac{\sigma_{12}\sigma_{23}}{\sigma_{22}\sigma_{13}}} \tag{6b}$$

$$\rho_{(T,3)} = \sqrt{\frac{\sigma_{13}\sigma_{23}}{\sigma_{33}\sigma_{12}}} \tag{6c}$$

It is worth observing that the square of correlation coefficients in Equations (6a)–(6c) are strictly related to the signal-to-noise-ratio of device ith (SNR_i), as in Mccoll et al. (2014):

$$SNR_i = \frac{\rho^2_{(T,i)}}{\left(1-\rho^2_{(T,i)}\right)} = \frac{\beta_i^2\sigma_T^2}{\sigma^2_{\varepsilon_i}} \tag{7}$$

where σ_T^2 is the variance of the unobserved true quantity. Thus, Equation (7) allows for transforming the correlation coefficients of measurements X_i with the unobserved truth T into the SNR_i, which better highlights the differences in the various measuring systems, especially in cases of high values of $\rho^2_{(T,i)}$. The P-TC has been applied to our dataset through a MATLAB code (Alemohammad et al., 2015b) available at https://github.com/HamedAlemo/MTC.

3.2 | Nonparametric triple colocation

The Nonparametric triple colocation (NP-TC) is a recently proposed method (Nearing et al., 2017b). It allows for the deriving of a statistic analogous to that of total error and total correlation as in Equations (5a)–(5c) and (6a)–(6c), but with the advantage, over P-TC, of not requiring the validity of assumptions (a), (b), and (e) in P-TC. NP-TC is based on probability information theory and it requires that the three measured quantities, X_i, $i = 1, 2, 3$, share some mutual information and that their probabilities, conditioned to the truth T, are independent of each other. The NP-TC theory is based on the statistical concept of information content (I) of a random variable X_i:

$$I(X_i) = -\ln\left[p(X_i)\right] \tag{8}$$

where $p(\cdot)$ indicates a probability. The case $p(X_i) = 1$ describes a fully expected observation, and consequently, produces no information, that is, $I(X_i) = 0$. The NP-TC is based on the entropy (H) of variable X_i, conditioned to the the unobserved truth T:

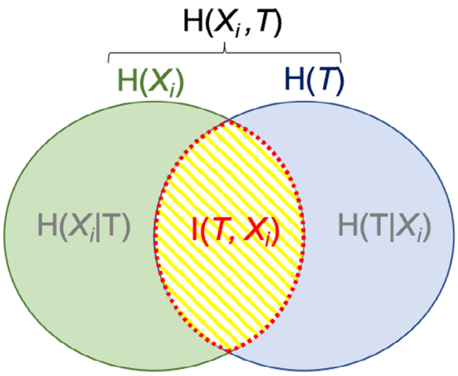

FIGURE 1 Graphical representation of the entropy of X_i, $H(X_i)$, and T, $H(T)$, joint entropy, $H(X_i,T)$, conditional entropies, $H(X_i|T)$, and $H(T|X_i)$ and mutual information, $I(T;X_i)$

$$H(X_i|T) = E\{I(X_i|T)\}. \tag{9}$$

$H(X_i|T)$ is a key quantity in NP-TC, since it represents the average information content (or variability) of X_i that is not caused by the intrinsic variability of T but, rather, is caused by the random error ε_i. In other words, $H(X_i|T)$ is the residual uncertainty amount (or, equivalently, the amount of randomness) of X_i for a given T. It is analogous to the squared errors in Equations (5a)–(5c) in the P-TC and the graphical interpretation is in Figure 1. On the other hand, the extension of Equation (8) in terms of the joint information content of X_i and T, yields:

$$I(T,X_i) = H(X_i) - H(X_i|T) \tag{10}$$

From Figure 1, it is intuitive to interpret $I(T;X_i)$ as the measure of the mutual dependence between T and X_i or, in other terms, the shared information content between the two variables. The normalization $I(T,X_i)\, H(X_i)$ produces a quantity that ranges in [0,1] and it is directly comparable with the squared correlation coefficients between the unobserved truth and X_i in Equations (6a)–(6c) for $i = 1, 2, 3$ in the P-TC case. Note that the first and second terms in Equation (7) hold also for NP-TC, being $H(X_i)$ referable to a signal plus noise term, whereas the term $H(X_i|T) = H(X_i) - I(T;X_i)$ can be thought as a purely noise term.

The implementation of NP-TC is carried out using the publicly available code on GithHub (Nearing et al., 2017a) at https://github.com/greyNearing/triple_collocation.

3.3 | Dual colocation

Dual colocation (DC) is the more common approach used to compare measuring systems pairwise. In this case, one measuring system (such as X_j) is assumed as the reference (i.e., error free), and, provided the error orthogonality holds, the standard deviation of the difference $d_{i,j} = X_i - X_j$ is:

$$\sigma_{d_{i,j}} = \sqrt{<\left(d_{i,j} - <d_{i,j}>\right)^2>} = \sqrt{(\beta_i - 1)^2\sigma_T^2 + \sigma_{\varepsilon_i}^2} \tag{11}$$

Note that in $\sigma_{di,j}$, the intrinsic variability of the true precipitation, σ_T^2, and the measurement error, $\sigma_{\varepsilon_i}^2$, are entangled together, thus making the characterization of ε_i alone not obvious (Duan et al., 2021). The special case $\sigma_{d_{i,j}} \approx \sigma_{\varepsilon_i}$, is verified only under the assumptions of linearity, error orthogonality, $\beta_i = 1$, and error free in the reference, X_j, which are limiting assumptions of the same order of strictness as for P-TC and NP-TC (Gruber et al., 2015).

4 | DESIGN OF INPUT TRIPLET AND PRE-PROCESSING

In this section, we briefly describe the set-up for P-TC, NP-TC, and DC method's implementation. Hereafter, the accumulated precipitation in (mm) over a time period ΔT, collected by the ith device, is labeled as $P_i^{\Delta T}$. Our pre-processing is subdivided into several steps.

Step 1 Rain rates $R_{\mathrm{THCD}}^{1\,\mathrm{min}}$ and $R_{\mathrm{2DVD}}^{1\,\mathrm{min}}$ ($\mathrm{mm\,h^{-1}}$) in Equations (1) and (2) are multiplied by 1/60 factor to transform them into rain accumulations $P_{\mathrm{THCD}}^{1\,\mathrm{min}}$ and $P_{\mathrm{2DVD}}^{1\,\mathrm{min}}$ (mm), respectively.

Step 2 $P_i^{1\,\mathrm{min}}$, with $i = $ 2DVD, THCD, RG, below a minimum sensitivity threshold P_{th}, are set to the no-rain value. P_{th} is set to that of RG (0.01 mm) so that the uneven detection capability of the three studied devices does not come into play, and detection errors caused by a lack of sensitivity, especially in RG, are not considered in our analysis.

Step 3 $P_i^{1\,\mathrm{min}}$ time series are integrated to the desired time periods ($\Delta t = 1$, 3, 6, 12, and 24 h). For 1 h integration, $P_i^{1\,\mathrm{min}}$ is integrated over contiguous hours, whereas for larger integration times, the integration extremes coincide with a Δt-wide sliding window, which is moved forward in time at step of 1 h, so that the accumulated precipitation for $\Delta t > 1$ h is updated constantly at every hour. This choice tends to preserve the total number of samples as the accumulation period increases, thus guaranteeing the statistical robustness of the final outcome. Since log-transformation requires data to be strictly

TABLE 1 Error standard deviation (ln(mm))/correlation coefficient of the three measuring systems obtained by P-TC (Equations (5a)–(5c) and (6a)–(6c)) in terms of accumulated precipitation $P_i^{\Delta t}$. The last column lists the relative difference (%) between error standard deviation values for 2DVD and THCD[a]. The last row is the signal-to-noise ratio (SNR) of device ith (dB)

Integration time (Δt)	2DVD	THCD	RG	Relative difference (%)
1 h	0.125/0.997	0.128/0.997	0.294/0.976	−2.300
3 h	0.126/0.997	0.129/0.997	0.299/0.977	−2.262
6 h	0.126/0.997	0.129/0.997	0.305/0.978	−2.453
12 h	0.127/0.998	0.130/0.997	0.313/0.980	−2.463
24 h	0.125/0.998	0.131/0.998	0.320/0.982	−4.509
SNR (dB)	22.8	22.6	13.6	

[a]Relative difference (q_1, q_2) (%) $= 100(q_1 - q_2)/q_2$.

positive, we adopt the same approach used in Alemohammad et al. (2015a) and in Massari et al. (2017) by removing hourly time slots with null precipitation.

It should be pointed out that removing zeros could shorten the sample size too much, compromising the stability of the TC results. In our case, the dataset is well populated, and the application of a moving window to determine the cumulative rainfall, enables us to circumvent such issue. However, we also tested the classical precipitation accumulation technique, in which the accumulation periods are next to each other, and verified similar results.

5 | RESULTS AND DISCUSSIONS

Results are obtained for P-TC, NP-TC, and DC formulations considering $X_i = \ln\left(P_i^{\Delta t}\right)$ with i = 2DVD or THCD or RG and Δt accumulation periods. Thereafter, Equations (5a)–(6c), (8)–(10), and (11) are implemented for P-TC, NP-TC, and DC, respectively. In the last case, 2DVD is considered as the reference truth.

In terms of P-TC, according to Table 1, the two disdrometers (THCD and 2DVD) have the best overall performance and their measuring systems present a similar error structure. The error STD estimated by P-TC is almost constant as the integration time increases and the relative error between 2DVD and THCD is below 5%. This result is in agreement with expectation since the measurement error should be independent of different integration periods. The correlation coefficient, ρ, (Table 1, second value in each entry) leads to similar conclusions, showing that the 2DVD and THCD rainfall products are closer to the underlying true signal than the RG. It is worth observing that the values of ρ, if read in terms of SNR using Equation (7), indicate that the noise effects are dominant for RG (average SNR = 13.6 dB) in contrast to disdrometers (average SNR = 22.6 dB and 22.8 dB for THCD and 2DVD, respectively). In addition, the relative sensitivity variation for

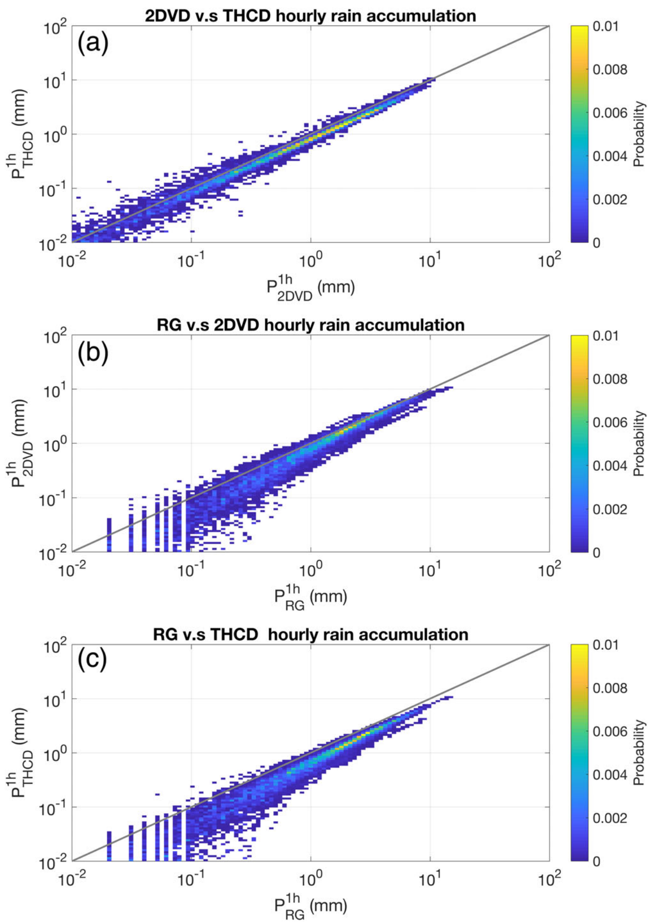

FIGURE 2 Scatter density plots of hourly rain accumulations P_i^{1h} from the three instruments analyzed: Thies Clima disdrometer (i = THCD), bi-dimensional video disdrometer (i = 2DVD) and rain gauge (i = RG). The regression lines are: $\ln\left(P_{2DVD}^{1h}\right) = 0.21 + 0.98\ \ln\left(P_{THCD}^{1h}\right)$; $\ln\left(P_{RG}^{1h}\right) = -0.32 + 1.17\ \ln\left(P_{2DVD}^{1h}\right)$; $\ln\left(P_{RG}^{1h}\right) = -0.52 + 1.16\ \ln\left(P_{THCD}^{1h}\right)$

the ith measuring system, with respect to the jth one, that is $\beta_{i,j} = (\beta_i - \beta_j)/\beta_j$, can be easily calculated recognizing that $\beta_i \sigma_T = \left(SNR_i \sigma^2_{\varepsilon_i}\right)^{1/2}$, with $\sigma^2_{\varepsilon_i}$ obtained by Equations (5a)–(5c) and β_i in Equation (4) defining the ith measuring system sensitivity. Using the values in Table 1, we found relative differences $\beta_{i,j}$ of the order of 21.0%, 20.3% and 0.6% for THCD vs. RG, 2DVD vs. RG and 2DVD vs. THCD, respectively. This suggests that disdrometers are more sensitive than RG in the order of 20%, whereas there are no significant differences between disdrometer types. The results achieved from the P-TC approach can be compared with those obtained by implementing the more typical DC method. Figure 2 shows, in each panel through the lens of the DC methodology, a joint bivariate probability of P_i^{1h}. It is evident that THCD tends to underestimate rainfall amounts as compared to the other devices, and it can be ascribed to an underestimation, by THCD, of midsize drops and an overestimation of small particles in agreement with what was already found in the literature. Table 2 quantifies the DC metric showing higher "error" STD than those obtained with P-TC. Nevertheless, DC indicates better performances for THCD than RG, consistently with what is obtained using P-TC. Finally, in terms of NP-TC, Table 3 confirms the RG as the noisiest instrument but shows, on average, a 4% higher relative error difference between 2DVD and THCD than what is obtained using P-TC. With regard to ρ (the second value in each Table 3 entry), the NP-TC and P-TC lead to similar conclusions, although NP-TC shows slightly smaller ρ which leads to average SNR = 5.4 dB, 4.5 dB and 3.3 dB for 2DVD, THCD and RG, respectively. These values suggest a larger noise component than what can be inferred by $SNRs$ from P-TC. Marginal differences in the values obtained by applying the two TC formulations may be due to some artifacts caused by strong assumptions and approximations in the P-TC (such as the imposition of an a-priori error structure or representativeness condition), although, overall, the two methods show a quite good agreement and indicate the 2DVD as the best performing device, closely followed by THCD and by RG. As last consideration, if we assume the NP-TC, thanks to its less restrictive constrains, as a reference method, the average error STD difference between dual colocation (Table 2) and NP-TC (Table 3) approach is found to be of the order of 40% and 75% for RG and THCD, respectively. Such values, provided the underlying assumptions are valid, might help quantifying the existing error gap between classical DC approaches and those based on NP-TC. As for the differences found between the RG OTT Pluvio^2 and disdrometers, the works of Colli et al. (2013, 2014, 2018) and Saha et al. (2021) highlight some issues related to the internal algorithm for the generation of OTT Pluvio^2 real-time product, and in its aerodynamic performances, which partially explains the lower performances found in our analysis for the OTT Pluvio^2.

TABLE 2 Error standard deviation (STD) (ln(mm))/Pearson correlation coefficient as in Equation (11) in the dual colocation mode

Integration time (Δt)	THCD vs 2DVD	RG vs 2DVD
1 h	0.180/0.994	0.442/0.973
3 h	0.181/0.994	0.444/0.974
6 h	0.182/0.995	0.444/0.976
12 h	0.182/0.995	0.444/0.978
24 h	0.182/0.996	0.442/0.980

6 | CONCLUSIONS

This work provides an error assessment of three in-situ precipitation sources, comparing the classical metric offered by the dual-colocation method, DC, with two formulations of the triple colocation approach, TC, namely parametric and nonparametric TC. The three precipitation devices considered are two disdrometer types (2DVD

TABLE 3 Error standard deviation (ln(mm))/correlation coefficient obtained by NP-TC in terms of accumulated precipitation $P_i^{\Delta t}$. The last column lists the relative difference (%) between error standard deviation for 2DVD and THCD[a]. The last row is the signal-to-noise ratio (SNR) of device ith (dB)

Integration time (Δt)	2DVD	THCD	RG	Relative difference (%)
1 h	0.709/0.868	0.733/0.856	0.793/0.820	−3.311
3 h	0.673/0.876	0.725/0.854	0.759/0.825	−7.105
6 h	0.650/0.883	0.705/0.860	0.749/0.827	−7.766
12 h	0.640/0.885	0.695/0.862	0.741/0.829	−7.869
24 h	0.627/0.889	0.688/0.864	0.731/0.834	−8.876
SNR (dB)	5.4	4.5	3.3	

[a]Relative difference (q_1, q_2) $(\%) = 100(q_1 - q_2)/q_2$.

and Thies Clima) and an OTT Pluvio^2 rain gauge. The test dataset was collected in Switzerland for a total of 607 days in very low-wind conditions, thus avoiding wind-induced effects in the three precipitation measuring systems being compared to each other. The results reveal both TC approaches implemented agree with each other in indicating closer error performances between 2DVD and THCD than RG in terms of rain accumulations, and identify 2DVD as the most accurate device, followed by THCD, and RG. We can conclude from this comparison that all three devices are able to provide accurate and close to each other precipitation estimates, even though a higher noise component has been observed in the OTT-Pluvio^2 measurements, which is likely related to device specific limitations. The more customary DC approach, confirms the results achieved. However, the NP-TC technique suggests that the actual error assigned to THCD and RG might be much larger than that estimated by the DC method. NP-TC gives the opportunity to investigate the performance of the three simultaneous measurements by relieving some strong assumptions which are required in the P-TC framework. For this reason, NP-TC can be thought to be more realistic than P-TC in real-world dynamical system and, therefore, it can be taken as a reference. As a general guideline, this work paves the way for a new prospective for characterizing the uncertainty of precipitation from in-situ ground based measuring systems. Future works will be oriented to apply the same error-verification approach distinguishing between various precipitation regimes and environmental conditions (such as wind) which introduce further sources of error.

AUTHOR CONTRIBUTIONS

Clizia Annella: Conceptualization; data curation; formal analysis; investigation; methodology; writing – original draft. **Vincenzo Capozzi:** Conceptualization; data curation; methodology; software; writing – original draft; writing – review and editing. **Giannetta Fusco:** Supervision; writing – review and editing. **Giorgio Budillon:** Funding acquisition; resources; supervision; writing – review and editing. **Mario Montopoli:** Conceptualization; investigation; methodology; supervision; visualization; writing – original draft.

ACKNOWLEDGEMENTS

This research was funded by AUTOSTRADE PER L'ITALIA (S.p.A.), Contract SAP n. 81004904, technical and scientific consulting contract with "Autostrade s.p.a." focused on the "Optimization of nowcasting methods based on X-band weather radar" and to the "Provision of a service of weather forecasting to support the management of highway traffic on the A1 section from Caianello to Naples, on the A30 from Caserta to Salerno and on the A16 section from Naples to Candela."

CONFLICT OF INTEREST

The authors declare no conflict of interest.

ORCID

Vincenzo Capozzi https://orcid.org/0000-0002-8279-9922

REFERENCES

Adirosi, E., Gorgucci, E., Baldini, L. & Tokay, A. (2014) Evaluation of gamma raindrop size distribution assumption through comparison of rain rates of measured and radar-equivalent gamma DSD. *Journal of Applied Meteorology and Climatology*, 53, 1618–1635.

Adirosi, E., Montopoli, M., Bracci, A., Porcú, F., Capozzi, V., Annella, C. et al. (2021) Validation of GPM rainfall and drop size distribution products through disdrometers in Italy. *Remote Sensing*, 13, 2081.

Alemohammad, S.H., McColl, K.A., Konings, A.G., Entekhabi, D. & Stoffelen, A. (2015a) Characterization of precipitation product errors across the United States using multiplicative triple collocation. *Hydrology and Earth System Sciences*, 19, 3489–3503.

Alemohammad, S. H., McColl, K. A., Konings, A. G., Entekhabi, D. and Stoffelen, A. (2015b) HamedAlemo/MTC. https://github.com/HamedAlemo/MTC.

Angulo-Martínez, M., Beguería, S., Latorre, B. & Fernández-Raga, M. (2018) Comparison of precipitation measurements by OTT Parsivel^2 and Thies LPM optical disdrometers. *Hydrology and Earth System Sciences*, 22, 2811–2837.

Atlas, D., Srivastava, R.C. & Sekkon, R.S. (1973) Doppler radar characteristics of precipitation at vertical incidence. *Reviews of Geophysics and Space Physics*, 2, 1–35.

Caires, S. & Sterl, A. (2003) Validation of ocean wind and wave data using triple collocation. *Journal of Geophysical Research: Oceans*, 108, 3098.

Capozzi, V., Annella, C., Montopoli, M., Adirosi, E., Fusco, G. & Budillon, G. (2021) Influence of wind-induced effects on laser disdrometer measurements: analysis and compensation strategies. *Remote Sensing*, 13, 3028.

Chinchella, E., Cauteruccio, A., Stagnaro, M. & Lanza, L.G. (2021) Investigation of the wind-induced airflow pattern near the thies LPM precipitation gauge. *Sensors*, 21, 4880.

Thies Clima (2015) Instruction for use. Laser precipitation monitor Göttingen: Adolf Thies GmbH & Co. KG.

Colli, M., Lanza, L. & La Barbera, P. (2013) Performance of a weighing rain gauge under laboratory simulated time-varying reference rainfall rates. *Atmospheric Research*, 131, 3–12.

Colli, M., Lanza, L., La Barbera, P. & Chan, P. (2014) Measurement accuracy of weighing and tipping-bucket rainfall intensity gauges under dynamic laboratory testing. *Atmospheric Research*, 144, 186–194.

Colli, M., Pollock, M., Stagnaro, M., Lanza, L., Dutton, M. & O'Connell, E. (2018) A computational fluid-dynamics assessment of the improved performance of aerodynamic rain gauges. *Water Resources Research*, 54, 779–796.

Duan, Z., Duggan, E., Chen, C., Gao, H., Dong, J. & Liu, J. (2021) Comparison of traditional method and triple collocation analysis for evaluation of multiple gridded precipitation products across Germany. *Journal of Hydrometeorology*, 22, 2983–2999.

Fehlmann, M., Rohrer, M., von Lerber, A. & Stoffel, M. (2020a) Automated precipitation monitoring with the Thies disdrometer: biases and ways for improvement. *Atmospheric Measurement Techniques*, 13, 4683–4698.

Fehlmann, M., Rohrer, M., von Lerber, A. and Stoffel, M. (2020b) Data for journal article: "automated precipitation monitoring with the Thies disdrometer: biases and ways for improvement". https://doi.org/10.5281/zenodo.3895297.

Gruber, A., Su, C.H., Zwieback, S., Crow, W., Dorigo, W. & Wagner, W. (2015) Recent advances in (soil moisture) triple collocation analysis. *International Journal of Applied Earth Observation and Geoinformation*, 45, 200–211.

Johannsen, L.L., Zambon, N., Strauss, P., Dostal, T., Neumann, M., Zumr, D. et al. (2020) Comparison of three types of laser optical disdrometers under natural rainfall conditions. *Hydrological Sciences Journal*, 65, 524–535.

Kathiravelu, G., Lucke, T. & Nichol, S.P. (2016) Rain drop measurement techniques: a review. *Water*, 8, 29.

Kruger, A. & Krajewski, W. (2002) Two-dimensional video disdrometer: a description. *Journal of Atmospheric and Oceanic Technology*, 19, 602–617.

Lanzinger, E., Theel, M. and Windolph, H. (2006) Rainfall amount and intensity measured by the Thies laser precipitation monitor. Geneva, Switzerland: WMO Technical Conference on Meteorological and Environmental Instruments and Methods of Observation (TECO-2006).

Larsen, M.L. & Blouin, C.K. (2020) Refinements to data acquired by 2-dimensional video disdrometers. *Atmosphere*, 11, 855.

Larsen, M.L., Kostinski, A.B. & Jameson, A.R. (2014) Further evidence for superterminal raindrops. *Geophysical Research Letters*, 41, 6914–6918.

Li, C., Tang, G. & Hong, Y. (2018) Cross-evaluation of ground-based, multi-satellite and reanalysis precipitation products: applicability of the triple collocation method across Mainland China. *Journal of Hydrology*, 562, 71–83.

Li, Z., Chen, M., Gao, S., Hong, Z., Tang, G., Wen, Y. et al. (2020) Cross-examination of similarity, difference and deficiency of gauge, radar and satellite precipitation measuring uncertainties for extreme events using conventional metrics and multiplicative triple collocation. *Remote Sensing*, 12, 1258.

Marzano, F.S., Cimini, D. & Montopoli, M. (2010) Investigating precipitation microphysics using ground-based microwave remote sensors and disdrometer data. *Atmospheric Research*, 97, 583–600.

Massari, C., Crow, W. & Brocca, L. (2017) An assessment of the performance of global rainfall estimates without ground-based observations. *Hydrology and Earth System Sciences*, 21, 4347–4361.

Mccoll, K., Vogelzang, J., Konings, A., Entekhabi, D., Piles, M. & Stoffelen, A. (2014) Extended triple collocation: estimating errors and correlation coefficients with respect to an unknown target. *Geophysical Research Letters*, 41, 6229–6236.

Nearing, G. S., Yatheendradas, S., Crow, W. T., Bosch, D. D., Cosh, M. H., Goodrich, D. C., Seyfried, M. S. and Starks, P. J. (2017a) grey-nearing/triple_collocation. https://github.com/grey-nearing/triple_collocation.

Nearing, G.S., Yatheendradas, S., Crow, W.T., Bosch, D.D., Cosh, M.H., Goodrich, D.C. et al. (2017b) Nonparametric triple collocation. *Water Resources Research*, 53, 5516–5530.

OTT HydroMet GmbH. (2019) Operating instructions: OTT Pluvio^2 precipitation gauge. Document number 70.040.000.B.E 01-0116. Available at: https://www.ott.com/download/operating-instructions-precipitation-gauge-ott-pluvio2-1/ (last access: 01 June 2022).

Park, S.G., Kim, H.L., Ham, Y.W. & Jung, S.H. (2017) Comparative evaluation of the OTT PARSIVEL 2 using a collocated two-dimensional video disdrometer. *Journal of Atmospheric and Oceanic Technology*, 34, 2059–2082.

Raupach, T.H. & Berne, A. (2015) Correction of raindrop size distributions measured by Parsivel disdrometers, using a two-dimensional video disdrometer as a reference. *Atmospheric Measurement Techniques*, 8, 343–365.

Saha, R., Testik, F. & Testik, M. (2021) Assessment of OTT Pluvio^2 rain intensity measurements. *Journal of Atmospheric and Oceanic Technology*, 38, 897–908.

Tapiador, F.J., Turk, F.J., Petersen, W., Hou, A.Y., García-Ortega, E., Machado, A.T. et al. (2012) Global precipitation measurement: methods, datasets and applications. *Atmospheric Research*, 104, 70–97.

Thurai, M. & Bringi, V.N. (2005) Drop axis ratios from a 2D video disdrometer. *Journal of Atmospheric and Oceanic Technology*, 22, 966–978.

Tian, Y., Huffman, G., Adler, R., Tang, L., Sapiano, M., Maggioni, V. et al. (2013) Modeling errors in daily precipitation measurements: additive or multiplicative? *Geophysical Research Letters*, 40, 2060–2065.

Tokay, A., Kruger, A. & Krajewski, W. (2001) Comparison of drop size distribution measurements by impact and optical disdrometers. *Journal of Applied Meteorology*, 40, 2083–2097.

World Meteorological Organization. (2018) Measurement of meteorological variables. In: *Guide to instruments and methods of observation*, Vol. 1. WMO: Geneva, Switzerland.

Yilmaz, M.T. & Crow, W. (2014) Evaluation of assumptions in soil moisture triple collocation analysis. *Journal of Hydrometeorology*, 15, 1293–1302.

How to cite this article: Annella, C., Capozzi, V., Fusco, G., Budillon, G., & Montopoli, M. (2022). Error investigation of rain retrievals from disdrometer data using triple colocation. *Atmospheric Science Letters*, e1127. https://doi.org/10.1002/asl.1127